Chemical Engineering Journal 159 (2010) 170–181

Contents lists available at ScienceDirect

Chemical Engineering Journal

journal homepage: www.elsevier.com/locate/cej

# Reset compensation for temperature control: Experimental application on heat exchangers

Angel Vidal, Alfonso Baños*

*Department of Informática y Sistemas, University of Murcia, 30100 Campus de Espinardo, Murcia, Spain*

ARTICLE INFO

*Article history:*
Received 6 November 2009
Received in revised form 15 February 2010
Accepted 16 February 2010

*Keywords:*
Reset control
Temperature problem
Heat exchanger
PID

ABSTRACT

This work aims at improving the control of an industrial heat exchanger by using reset compensation. The goal is investigating the potentials of a hybrid compensator previously developed by the authors, the PI+CI reset compensator, in the robust control when significant uncertainty is present. To this end, a PI+CI compensator has been designed by using a two step method: firstly, a robust base PI compensator is tuned by using the Quantitative Feedback Theory to satisfy (robust) relative stability and tracking specifications; and secondly, a partial reset action is added to the base lineal PI compensator to improve transitory response. In addition, a PI compensator is tuned by using the Internal Model Control for comparison purposes. Finally, the reset conditions are simply modified in the PI+CI compensator to overcome the effect of the dominant time delay over the reset action, through the introduction of a reset band which can have fixed or variable values along the time.



## 1. Introduction

Temperature control is a common problem in the process industry, such as power generation, chemical plants, refrigeration and food processing among others. This temperature problem arises from the large process uncertainty and the different operation conditions which are carried out during the whole process. For example, in batch reactors the temperature has to be adjusted to an optimal temperature profile in spite of the drastic changes in set points with the goal of obtaining a specific product with desired properties [3,14,27]. In other applications, such as thermal treatments in heat exchangers, the outlet temperature has to be maintained in a particular set-point for a wide variety of products and different operation points in order to destroy harmful microorganisms and optimise food quality factors [5,19,28]. Because of these particularities, thermal control is difficult to achieve with conventional PID controllers. Since variable operating conditions are carried out, the parameters of the PID controller require frequent returning to adjust them to these different operating conditions. Some works deal the temperature control problem by using adaptive model predictive control [1–3,24,27]. In this kind of works it is necessary a high accuracy between the model used for controller design and the process model to achieve a good control performance. Other works are focused on the use of the Quantitative Feedback Theory (QFT) to tune a robust controller which takes into account the thermal process uncertainty [8,15]. Precisely, this latter technique is the one used in this work for the control of an industrial heat exchanger.

QFT is a robust control technique that is especially well suited for control problems with large plant uncertainty. It has been developed since the early sixties following the seminal works of Horowitz [21], and it has been successfully applied to scalar/multivariable, LTI/nonlinear and time varying, single loop/multiloop systems [22,23]. The basic idea of this technique consists of using a family of linear time invariant (LTI) plants obtained by local linearization of the heat exchanger nonlinear dynamic around different operation points, following the method developed in [11]. The result is a robust compensator that guarantees a specified worst-case behavior for all the considered operation points. In general, the robustness and performance has to be balanced due to fundamental limitations of the resulting LTI compensator, being this the main motivation of the present work, where a type of nonlinear/hybrid control referred to as reset control is investigated with the goal of improving performance without sacrificing robustness.

Reset compensation was one of the first attempts to overcome fundamental limitations of LTI control systems. Its development was initiated fifty years ago with the work of Clegg [16], that introduced a nonlinear integrator based on a reset action. Basically, the Clegg integrator (CI) consists of an integrator whose output

*Abbreviations:* CI, Clegg integrator; FOPTD, first order plus time delay; IAE, integral absolute error; IMC, internal model control; ITAE, integral time absolute error; LTI, linear time invariant; PI, proportional integral; PRBS, pseudorandom binary sequence; QFT, Quantitative Feedback Theory.

* Corresponding author.
*E-mail addresses:* anvisa222@hotmail.com (A. Vidal), abanos@um.es (A. Baños).

1385-8947/$ – see front matter © 2010 Elsevier B.V. All rights reserved.
doi:10.1016/j.cej.2010.02.033

**Nomenclature**

| | |
|---|---|
| $A$ | area for heat transfer ($m^2$) |
| $\Delta T$ | temperature difference (°C) |
| $\Delta T_{lm}$ | log mean temperature difference (°C) |
| $\mathcal{B}_\delta^f$ | fixed reset band surface |
| $\mathcal{B}_h^v$ | variable reset band surface |
| $C$ | compensator model |
| $d$ | perturbation signal |
| $\delta$ | fixed reset band value |
| $e$ | error signal |
| $E$ | error amplitude |
| $h$ | time delay of the heat transfer model (s) |
| $k$ | gain of the heat transfer model |
| $k_p$ | proportional gain of a PI/PI+CI compensator |
| $\lambda$ | time constant of the desired closed loop response (s) |
| $\mathcal{M}$ | reset surface |
| $n$ | noise signal |
| $P(s)$ | heat exchanger model |
| $p_{\rm reset}$ | reset ratio of a PI+CI compensator |
| $q$ | heat transfer rate (kcal/h) |
| $r$ | reference signal |
| $t_k$ | $k$ th reset time (s) |
| $T_{\rm in}$ | product temperature at the heat exchanger inlet (°C) |
| $T_{\rm out}$ | product temperature at the heat exchanger outlet (°C) |
| $T_s$ | steam temperature (°C) |
| $\tau$ | time constant of the heat exchanger model (s) |
| $\tau_i$ | integral time constant of a PI/PI+CI compensator (s) |
| $u$ | control signal |
| $U$ | overall heat transfer coefficient (kcal/°C $m^2$) |

is set to zero whenever its input is zero. Therefore, a faster system response without excessive overshooting may be expected, and the limitation of its LTI counterpart is avoided. Although several other nonlinear compensators were developed, all based on describing function analysis, it is in a series works by Horowitz [22,23], where reset control systems were impulsed by introducing the first order reset element (FORE).

Reset compensation is simply implemented just by resetting the state (or part of it) of a feedback LTI compensator (referred to as the base LTI compensator) at every instant in which its input is zero. Usually the design of the reset control is strongly dependent on a proper election of the base LTI control system. A common approach is to design the base LTI system to be stable and to fulfill some performance specifications, and then including reset over some compensator states to improve performance and robustness. However, this method should be carefully applied, since it is well known [12,13] that the reset action may destabilize a base LTI control system. Thus, reset control may be used to overcome fundamental limitations of LTI control systems, but it may work worse than its base LTI system. In previous works by authors [9,10] a reset compensator based on a PI compensator has been introduced, it consists of a PI compensator plus a Clegg integrator and it has been referred to as PI+CI compensator. Other applications of reset compensation can be found in [20], where a reset control of a single stage hard disk drive servo system is performed, in [34], where a piezoelectric positioning stage is used, and in [17], where the reset compensation is applied on teleoperation.

In [9,10] tuning rules of the PI+CI compensator for first and second order systems with time delay has been developed. In the present work, this PI+CI reset controller is tuned by using QFT and

**Fig. 1.** Pilot plant.

applied on the temperature control of an industrial heat exchanger. In Section 2, the heat exchanger to be controlled is defined and modelled for different operation points; in addition the PI+CI controller is also studied as a type of reset controllers. In Section 3, the QFT design method is applied upon the modelled heat exchanger with the goal of getting a well-tuned PI+CI controller. In addition, a PI controller is tuned via Internal Model Control (IMC) for comparison purposes. Finally, the reset controller response is improved just by modifying the controller reset condition in two different ways.

## 2. Materials and methods

The temperature problem will be studied in this work by using an industrial heat exchanger, commonly used in food industries for thermal treatments. For that purpose, the temperature process will be modeled through pseudorandom binary sequence (PRBS) experiments and step test application. PI+CI compensation will be used to fix the outlet temperature at a desired value with minimum performance indexes, such as the integral absolute error (IAE).

### *2.1. Industrial equipment*

The heat exchanger used in this work is part of a pilot plant which has been designed for food industry applications. This pilot plant can be seen in Fig. 1.

This HRS UNICUS double tube heat exchanger consists of a 3 m long tube within another one in parallel flow. That is to say, the product flows through the inner tube in parallel to the serviced fluid which flows through the annulus between the inner and the outer tube. In addition, the shell and tube heat exchanger has scraper bars fitted in each interior tube whose movement mixes the fluid and cleans the heat exchange surface. This also keeps heat transfer high and makes cleaning tasks easier in food industries. The physical details of this heat exchanger are shown in Table 1.

The product is pumped from the storage tank up to the heat exchanger by an industrial helicoidal impeller pump. Two resistance thermometers used as thermocouples are placed at both the inlet and the outlet of the inner tube of the heat exchanger for tem-

**Table 1**
Physical details of the industrial heat exchanger.

| | |
|---|---|
| Number of inner tubes | 1 |
| Shell diameter | 104 mm |
| Inner tube diameter | 76.2 mm |
| Type of flow | Parallel |
| Material | Stainless steel |
| Tubes lenght | 3000 mm |

**Fig. 2.** Electropneumatic globe valve.

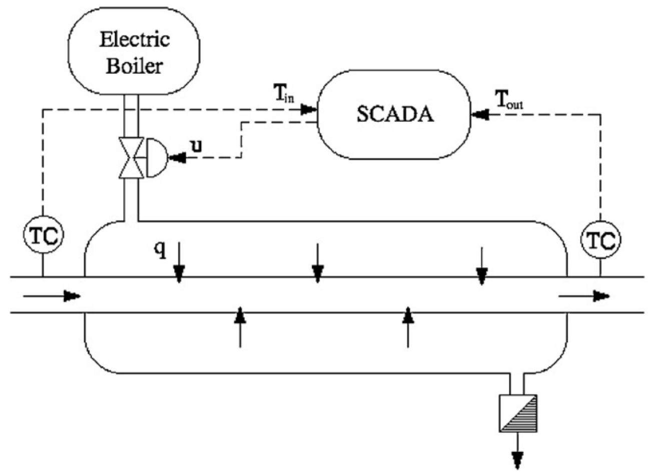


**Fig. 3.** Industrial heat exchanger control.

perature measurements. Specifically, these thermocouples consist of PT-100 (Wika) which are able to measure temperature in a range between 0 ◦ C and 150 ◦C, with a bias smaller than 0.4 ◦ C and a precision, or standard deviation, equals to 0.3 ◦ C as maximum.

The product is heated in the inner tube from the saturated steam condensation at the shell side. The rate of heat transfer depends on the temperature difference between the cold and hot fluids, in such a way that the higher this difference is, the faster the heat is transferred. Therefore, the heat transfer rate, $q$ in kcal/h, is expressed through the following equation:

$$q = UA\Delta T_{\rm lm} \tag{1}$$

where $A$ is the area for heat transfer in $m^2$, $U$ is the overall heat transfer coefficient, kcal/◦C m$^2$, and $\Delta T_{\rm lm}$ is the log mean temperature difference in ◦C.This temperature difference is the average value between the hot and cold fluids at the inlet and outlet of the heat exchanger and it is expressed as follows:

$$\Delta T_{\rm lm} = \frac{(T_{\rm s} - T_{\rm out}) - (T_{\rm s} - T_{\rm in})}{\ln(T_{\rm s} - T_{\rm out})/(T_{\rm s} - T_{\rm in})} \tag{2}$$

where $T_{\rm s}$ is the steam temperature in ◦ C and $T_{\rm in}$ and $T_{\rm out}$ are the product temperatures at the inlet and outlet of the heat exchanger respectively.

The saturated steam is generated in an electrical boiler of 12 kW of power which generates 16 kg of steam per hour at a pressure which oscilates between 4.3 and 5 bar. These pressure drops will be taken into account as a perturbation, $d$, in the control scheme (see Fig. 6). The control signal will be precisely the steam flow rate, which will be controlled through the aperture (expressed in %) of an electropneumatic globe valve placed just before the shell inlet in the heat exchanger, as seen in Fig. 2. This control valve is a type 3321 globe valve from Samson (DN15, KVS 1.6 and PN16) which is equipped with an electropneumatic actuator with integrated i/p positioner.

The thermocouples and the control valve are connected through an ABB automaton to a data acquisition system, where the ABB SCADA is installed for monitoring and control purposes, as it can be seen in Fig. 3. The ABB SCADA system reads both the inlet and outlet temperatures, $T_{\rm in}$ and $T_{\rm out}$, and from this temperature difference, $\Delta T = T_{\rm out} - T_{\rm in}$, the control system provides the corresponding electropneumatic globe valve aperture, $u$ in %, in order to reach the desired reference temperature.

The industrial heat exchanger is modelled by using as product a water flow rate of 250 L/h. The identification is done through pseudorandom binary sequence (PRBS) experiments and step test application. On one hand, the heat exchanger models are obtained by first order approximation describing the response of the temperature along the heat exchanger to several step changes of valve aperture. Specifically, this identification was done by opening the control valve from 10 up to 25% in 5% steps and then by closing the control valve up to 10% by using again 5% steps, as it can be seen in Fig. 4.

In addition, on the other hand, the PRBS experiments are also done to model the heat exchanger. These experiments [25] consists of doing different experiments by using the control signal as the input, which will have an spectrum with significative components in some regions of interest. Then, the different responses data are used for getting an uncertain parametric model. One example of a PRBS experiment is shown in Fig. 5 for a valve aperture between 10 and 15%.

With these modeling experiments, the heat exchanger can be represented by a set of first order plus time delay (FOPTD) transfer functions, given by

$$P_{a-b\%}(s) = \frac{k_{a-b\%}}{\tau_{a-b\%}s + 1} e^{-h_{a-b\%}s} \tag{3}$$

For each valve aperture change, from $a$% to $b$%, a heat exchanger model is obtained, given in Table 2. From these models, the heat exchanger uncertainty is expressed in parametric form as $k_{a-b\%} \in [0.31, 0.40]$, $\tau_{a-b\%} \in [80, 114]$ and $h_{a-b\%} \in [50, 88]$.

Note that the control valve is just opened up to 25% because a higher aperture would produce a pressure drop inside the electric boiler, with the consequent temperature drop at the outlet of the heat exchanger.

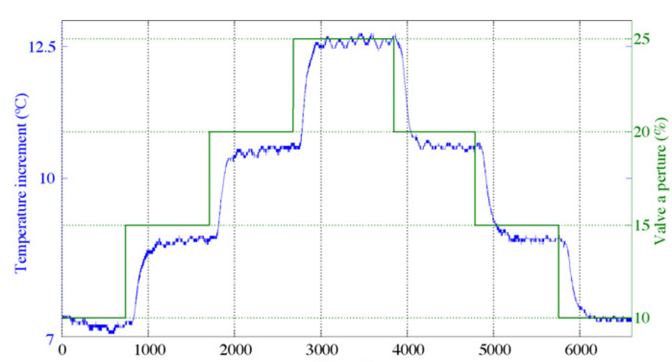


**Fig. 4.** Heat exchanger identification.

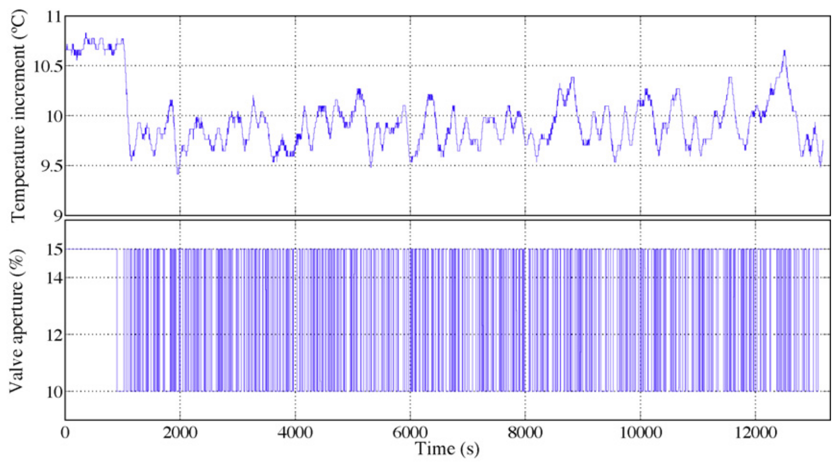


**Fig. 5.** PRBS experiment.

**Table 2**
Heat exchanger uncertainty.

| Plant $P_{a-b\%}$ | Gain $k_{a-b\%}$ | Time constant $\tau_{a-b\%}$ (s) | Time delay $h_{a-b\%}$ (s) |
|---|---|---|---|
| $P_{10-15\%}$ | 0.32 | 87 | 88 |
| $P_{15-20\%}$ | 0.35 | 82 | 83 |
| $P_{20-25\%}$ | 0.40 | 80 | 65 |
| $P_{25-20\%}$ | 0.40 | 89 | 50 |
| $P_{20-15\%}$ | 0.35 | 95 | 76 |
| $P_{15-10\%}$ | 0.31 | 114 | 84 |

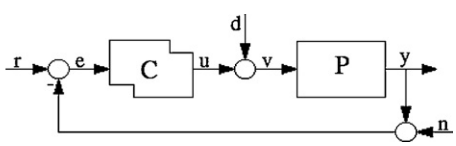

**Fig. 6.** Control scheme.

## 2.2. Methods

For control purposes, the control scheme used in this work can be seen in Fig. 6, where $P$ is the heat exchanger model and $C$ is the reset compensator which will be design with QFT. The signal $d$ is the perturbation introduced by the oscillations of the steam pressure inside the electric boiler and the signal $n$ refers to the noise introduced by the termocouples.

The reset compensator used in this work is the reset PI+CI controller. This kind of compensator can be interpreted as a PI controller with reset action on its integral term [9,10]. Specifically, a PI+CI controller is defined simply by adding a Clegg integrator (CI) [16] to a PI controller. In this perspective, the PI+CI controller will have three terms as shown in Fig. 7.

In this compensator, $k_p$ and $\tau_i$ are the proportional gain and the integral time constant of its counterpart PI compensator. The reset ratio $p_{\text{reset}}$ represents the part of the integral term over the reset action is applied, and it is used to set the partial reset on the integral term.

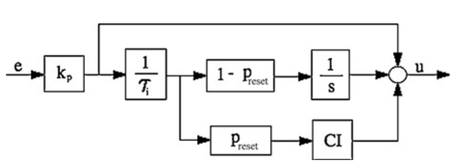

**Fig. 7.** PI+CI compensator structure.

It has been shown in [9,10] that this partial reset of the integral term results in an improvement on the transitory closed loop response, reducing the overshoot and settling time corresponding to the design without reset.

In the state-space, a PI+CI controller can be expressed by using two states, one corresponding to the integral term, an the other corresponding to the Clegg integrator term: $x_r = (x_i, x_{ci})^\top$, where $\top$ denotes transposition

$$C : \begin{cases} \dot{x}_r = B_r e, & e \neq 0 \\ x_r^+ = A_\rho x_r, & e = 0 \\ v = C_r x_r + D_r e \end{cases} \tag{4}$$

where the reset matrix, $A_\rho$, selects the state to be reset and $x_r^+$ or $x_r(t^+)$ is the value $x_r(t+\epsilon)$ with $\epsilon \to 0^+$. The matrices $B_r, A_\rho, C_r$ and $D_r$ are given by

$$B_r = \begin{pmatrix} 1 \\ 1 \end{pmatrix}, \quad A_\rho = \begin{pmatrix} 1 & 0 \\ 0 & 0 \end{pmatrix}$$
$$C_r = \frac{k_p}{\tau_i} \begin{pmatrix} 1 - p_{\text{reset}} & p_{\text{reset}} \end{pmatrix}, \quad D_r = k_p$$

Considering this controller and the heat exchanger model (3), the unforced closed loop system from Fig. 6 is expressed by the following impulsive differential equation

$$\begin{cases} \dot{x}(t) = Ax(t) + A_d x(t-h), & x(t) \notin \mathcal{M} \\ x(t^+) = A_R x(t), & x(t) \in \mathcal{M} \\ y(t) = Cx(t) \end{cases} \tag{5}$$

where the reset surface $\mathcal{M}$ is defined by

$$\mathcal{M} = \{x \in \mathbb{R}^n : Cx = 0\} \tag{6}$$

As it was remarked in [33], reset systems, such as (5), are prone to the presence of Zeno solutions. To avoid this kind of solutions, the notion of temporal regularization is used here in the same way it was already used in [33]. Therefore, to avoid Zeno solutions any implementation of the closed loop system (5) would require the time regularization as follows

$$\begin{cases} \dot{\tau}=1,\ \dot{x}(t)=Ax(t)+A_d x(t-h), & (x(t)\notin \mathcal{M})\vee(\tau\le\rho) \\ \tau^+=0,\ x(t^+)=A_R x(t), & (x(t)\in\mathcal{M})\wedge(\tau>\rho) \\ y(t)=Cx(t) \end{cases} \quad (7)$$

where $\rho$ is a finite positive scalar arbitrary small. As it was explained in [6], there exists a unique well-defined solution satisfying

$$x(t)=e^{A(t-t_k)}x(t_k)+\int_0^h e^{A(t-t_k-\tau)}A_d x(t_k+\tau-h)\,d\tau \quad (8)$$

for non resetting instants $t\in(t_k, t_{k+1})$, $k=0,1,\ldots$ and for a given initial condition. In addition, reset instants are given by

$$Cx(t_k)=0\wedge\rho>0 \quad (9)$$

and $t_{k+1}-t_k>\rho$, $k=0,1,\ldots$, is satisfied.

The stability of this kind of reset systems has already been studied in a previous work developed by the auhors [32]. In [32] the PI+CI compensator stability is studied by partitioning the state space into several regions with the goal of identifying the reset surface with a neighbouring region. Once the state space is partitioned, stability constrained conditions are given as several linear matrix inequalities by using Lyapunov techniques. Furthermore, the $\mathcal{S}$-procedure technique is applied on these constrained linear matrix inequalities to demonstrate the exponential stability of a PI+CI-based reset control system.

In the frequency domain, the stability of the reset closed loop system can be analyzed by using the describing function method. This method, in spite of being an approximation, has the advantage that delays can be taken into account in a quite natural way. The describing function of the PI+CI compensator can be obtained by adding the describing function of a Clegg integrator [16] to a PI controller as shown in Fig. 7. In that way, the describing function of a PI+CI controller is simply given by

$$D_{\text{PI+CI}}(j\omega)=k_p\left(1+\frac{1-p_{\text{reset}}}{\tau_i}\frac{1}{j\omega}+\frac{p_{\text{reset}}}{\tau_i}\frac{1.62}{\omega}e^{-j38.1^\circ}\right) \quad (10)$$

As it can be seen, the difference between a PI+CI controller and its counterpart PI is that the reset action will give extra phase lead of more than 50° over a (LTI) integrator [10,16]. This has been one of the main reasons to use PI+CI compensation in order to overcome fundamental limitations of LTI compensation.

The Quantitative Feedback Theory (QFT) will be used to tune a PI+CI compensator by taking into account the process uncertainties. QFT is a robust control technique that is especially well suited for control problems with large plant uncertainty. It has been developed since the early sixties by Prof. Horowitz and his collaborators [21], and it has been applied to scalar/multivariable, LTI/nonlinear and time varying, single loop/multiloop systems [22,23]. QFT works in the frequency domain, thus plant models can be derived from transfer functions (usually with parametric uncertainty) or directly by sets of frequency responses. QFT basically consists of several design steps

1. *Computation of templates*. A template represents, at a given frequency, the uncertainty of the plant. It is a region of the Nichols Plane, where each point is given by the phase and magnitude of a plants set element. For a set of working frequencies, the first design step consists of computing the templates set.
2. *Computation of boundaries*. Given (robust) stability and performance specifications, each template generates a boundary. If the nominal open loop gain avoids the boundaries, one boundary at every working frequency, then closed loop specifications are satisfied for all the plants considered in the template.
3. *Nominal open loop shaping*. Once the boundaries are computed, the next design step is to compute (shape) the open loop gain so that it fits them in some optimal way. In general, this is a hard computational problem that usually has been solved heuristically. Once the open loop gain is obtained, the feedback compensator is directly computed. In addition, a precompensator can be added to the feedback structure if tracking specifications have to be satisfied.

## 3. Results and discussion

In this section the same experiment in the industrial heat exchanger will be carried out with different controllers such as a linear PI one and a reset PI+CI compensator without and with modifications in its reset condition. The common experiment consists of setting a fixed product flow, 250 L/h as considered in the modeling procedure, and opening the control valve at 10%. When the steady-state temperature is reached at this control valve aperture, the reference temperature is increased and decreased by step changes with a magnitude of 2 °C. The maximum temperature increment between the inlet and outlet temperature will be equal to 6 °C, since a higher increment will produce a pressure drop in the electric boiler with the subsequent outlet temperature drop.

### 3.1. Linear compensation design

For comparison purposes, a linear PI controller is tuned by using a simple and robust technique, the Internal Model Control (IMC). This method consists of considering a known model of the process in order to get a desired closed loop response. For that purpose, the controller parameters will depend on the system parameters and on the time constant of the desired closed loop response, $\lambda$. Specifically, when the process is modeled as a FOPDT system (3) the controller takes the structure of a PI controller with the following parameters [31]

$$k_p=\frac{\tau}{k(\lambda+h)} \quad (11)$$

$$\tau_i=\tau \quad (12)$$

The value of the desired closed-loop time constant $\lambda$ can be chosen freely, but from (11) it has to be $-h<\lambda<\infty$ to get a positive and nonzero controller gain. In general, the optimal value of $\lambda$ should be determined by a trade-off between

1. Fast response and good disturbance rejection (small value of $\lambda$)
2. Stability and robustness (large value of $\lambda$)

Between the different ways of fixing the value of $\lambda$ which have been studied in the literature [26,29,30], the one given by [30] is used in this work. So, the value $\lambda$ is chosen to be equal to the time delay $\lambda=h$. This gives a reasonably fast response with good robustness margins. In this way the PI proportional gain (11) is given as

$$k_p=\frac{\tau}{2kh} \quad (13)$$

For the industrial heat exchanger modeled by (3)-Table 2, a nominal model has to be considered to tune the PI controller via IMC. In this work, the chosen model is the one in which the control valve is opened from 15% up to 20%

$$P_{15-20\%}=\frac{0.35}{82s+1}e^{-83s} \quad (14)$$

For this model, by using (13) and (12) the following PI parameters are obtained, $k_p=1.41$ and $\tau_i=82$ s. From now, this controller is going to be named as PI-IMC. The experiment explained previously has been carried out with this controller. That is, the control valve is opened at 10% until the steady-state is reached. The difference

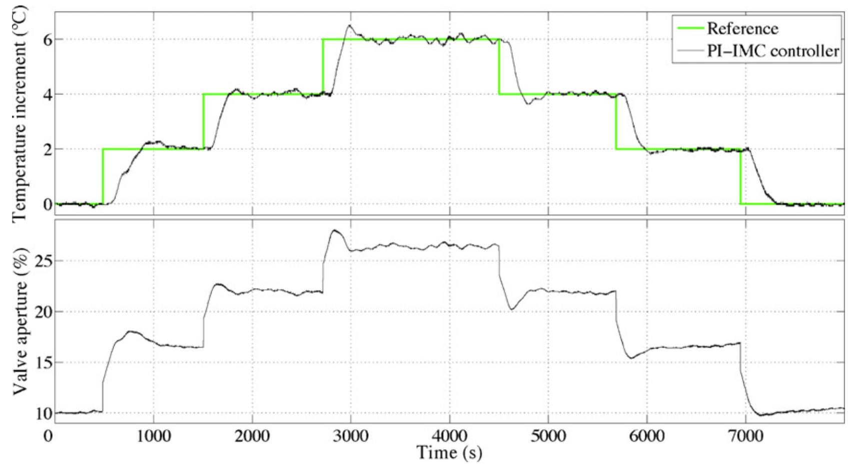


**Fig. 8.** Responses and control signals of PI controller tuned by IMC.

between the outlet and inlet temperatures, $\Delta T = T_{out} - T_{in}$, is taken as 0 °C. Then 2 ° C step changes are introduced into the reference temperature from 0 ° C up to 6 ° C and from this value up to 0 ° C again.

In Fig. 8 the temperature increments in the heat exchanger are shown together with the control signal, that is the control valve aperture. In both signals, it can be seen the noise introduced by the thermocouples and the perturbations due to the pressure drops occurred at the electric boiler. Note that the higher the control valve is opened the more oscillatory the response is at the steady-state. Regarding the control system, it can be seen that the PI-IMC controller is robust for all the reference changes. In addition, fast responses are obtained (rise time between 98 and 233 s) with hardly overshoot (between 4.5% and 26%).

### 3.2. Reset compensation design

The main goal of this work is to design a reset control system that guarantees both a robust and better performance than the one given by the PI controller. This better performance will consist of increasing the response velocity without increasing its overshoot. For that purpose the PI+CI controller is going to be used. As it was explained in Section 2.2, this reset controller is designed from a lineal PI controller just by adding a proper reset ratio $p_{reset}$. Since the PI-IMC hardly has overshoot, a faster base PI controller with more overshoot has to be tuned. Then, the PI+CI controller is tuned by adding a reset ratio to this faster base PI controller. As it was explained in Section 2.2, the Quantitative Feedback Theory (QFT) will be used to design this base LTI control system. Design specifications will be closed loop stability and tracking performance. In a second stage, this base PI compensator will be used to design the final reset control system.

#### 3.2.1. Base PI compensator tuning

The base PI controller will be tuned with QFT by following the design steps explained in Section 2.2. First of all, plant templates are computed by taking into account parametric uncertainty as given in (3)-Table 2, where the nominal plant is considered as

$$P_{15-20\%}(s) = \frac{0.35}{82s+1}e^{-83s} \qquad (15)$$

In this case, the templates are obtained for a wide set of working frequencies, specifically from 0.002 up to 0.02 rad/s.

Secondly, boundaries are computed for each frequency from design specifications by using the templates. Design specifications

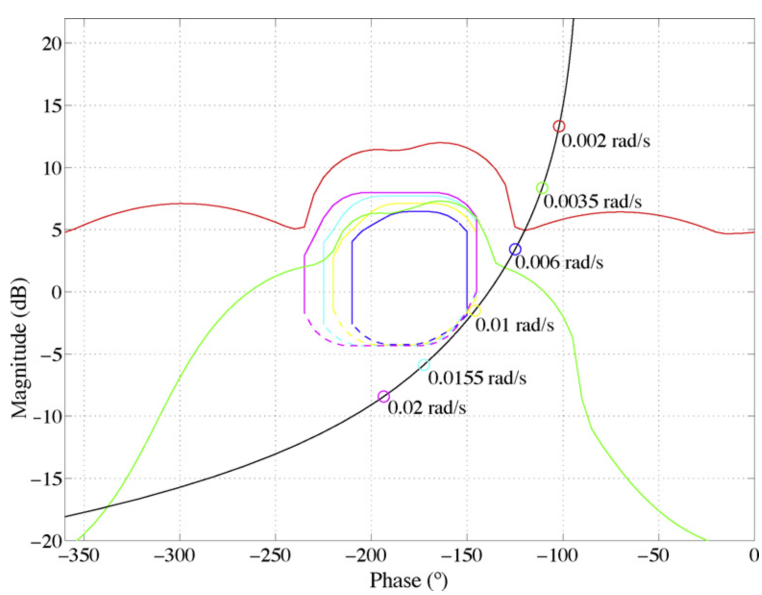


**Fig. 9.** Base PI open loop design.

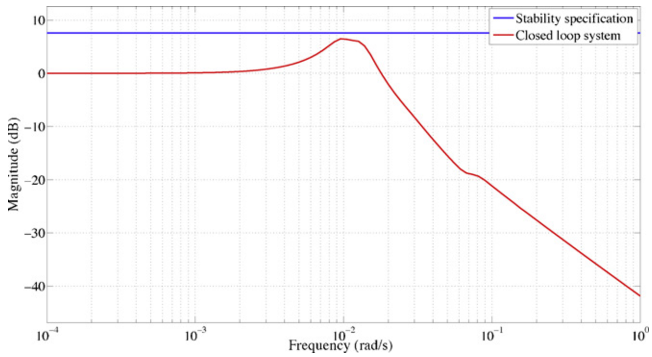


**Fig. 10.** Stability analysis.

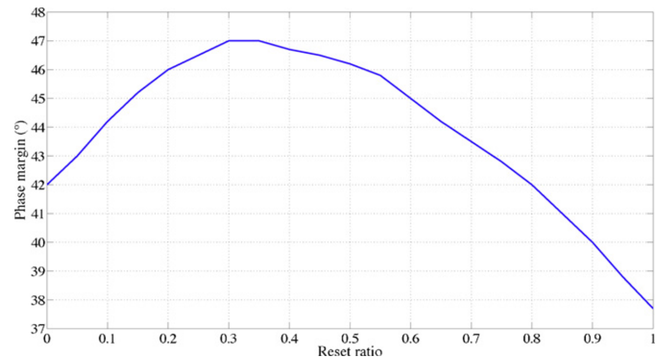


**Fig. 12.** Phase margin of PI+CI reset system for different values of $p_{\text{reset}}$.

will be a minimum (robust) phase margin of 24°, and desired tracking performance, such as a rise time between 45 and 180 s and a maximum overshoot between 7% and 75%.

Note that a relatively small phase margin has been specified for the base PI control system. In addition, note also that the response is specified to be faster and with more overshoot than the response obtained with the PI-IMC controller. These design specifications are considered due to the fact that the reset compensation will improve the minimum phase margin and will reduce the overshoot of the PI compensator without reducing its velocity.

The next step consists of shaping the nominal open loop. Here a PI controller is tuned by making the open loop gain fits both the stability and tracking boundaries. A shaping is shown in Fig. 9, corresponding to a proportional gain of $k_p = 1.6$ and an integral time constant of $\tau_i = 60$ s.

Finally, once the base PI compensator is tuned, a closed loop system analysis is done to ensure that the system fits the given stability and tracking specifications. This is usually referred as compensator validation in QFT. This analysis has to be done for a wider set of frequencies than the one used in the templates computation, and in this case, this set goes from 0.00001 up to 100 rad/s with a much bigger gridding. In Fig. 10, the stability analysis is shown, whereas the tracking analysis is done in Fig. 11.

As it can be seen, the designed closed loop system satisfies both stability and tracking specifications for every frequency. Therefore, the base PI compensator design is finished.

### 3.2.2. PI+CI reset compensator tuning

Once the base PI compensator has been designed, the obtained PI parameters are chosen as a part of the PI+CI parameters [10]. But, in addition, an additional parameter, the reset ratio ($p_{\text{reset}}$), must be tuned. For a proper election of this parameter it is important to note that for high values of $p_{\text{reset}}$ a worse closed loop response can be expected [9,10]. Here, the tuning rules derived in the above works are used to tuning this parameter for the nominal loop. The expected result is an increment of the phase margin and thus a better transitory response for the industrial heat exchanger.

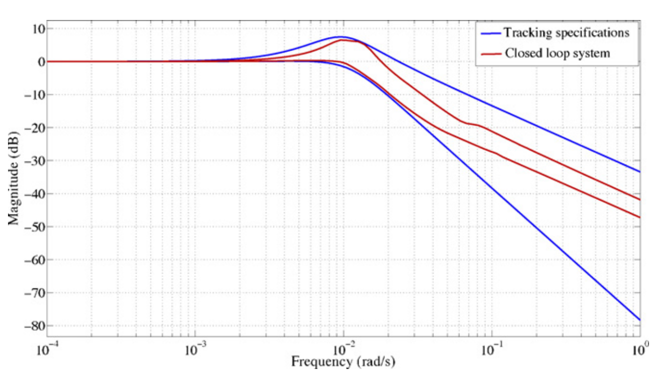


**Fig. 11.** Tracking analysis.

In Fig. 12 the phase margin system is drawn for different reset ratio values. As it can be seen, the phase margin increases from 42° ($p_{\text{reset}} = 0$, LTI system) up to 47° ($p_{\text{reset}} \in [0.30, 0.35]$).

In order to study the reset system performance, several values of reset ratio will be considered. Specifically, low reset ratio values will be taken to study the reset influence upon the system performance, $p_{\text{reset}} = 0.1$ and $p_{\text{reset}} = 0.2$. In addition, in order to reach the maximum phase, two additional reset ratio values are also considered, such as $p_{\text{reset}} = 0.3$ and $p_{\text{reset}} = 0.4$.

These PI and PI+CI controllers are used to control the already described heat exchanger. For this purpose the same experiment carried out with the PI-IMC controller is done again. Fig. 13 shows the temperature increment and the valve aperture when the PI and PI+CI compensations are used.

As it can be seen, all the control systems (for base PI and PI+CI compensation) are equal until the reset action is experimented. After reset, the PI+CI systems have the same or less first overshoot while the rest overshoots and undershoots are increased respected to the base PI system. This reset response is not the expected one, since the heat exchanger response under reset action is worse than the lineal one, and sometimes it has more overshoot and undershoot.

The integral absolute error (IAE) and the integral time absolute error (ITAE) are computed to evaluate the output control performance

$$\text{IAE} = \int_0^{\infty} |e(t)|\,\mathrm{d}t \tag{16}$$

$$\text{ITAE} = \int_0^{\infty} t|e(t)|\,\mathrm{d}t \tag{17}$$

which should be as small as possible.

These performance indexes confirm that the reset action makes the error increase and therefore the response gets worse. In addition, for comparison of results, phase margins are also computed in Table 3 for these compensators. These values show the extra phase lead given by the PI+CI compensator: for the PI controller the phase margin is 41° whereas for the PI+CI reset one the phase margin can be increased up to 47°.

The worse response under reset conditions, Fig. 13, is due to the fact that the effect of the reset action takes place after the crossing of the output with the reference, due to the existence of dominant time delays in the system. Therefore, in the next a simple modification of the reset PI+CI compensator will be investigated to significantly improve control system performance.

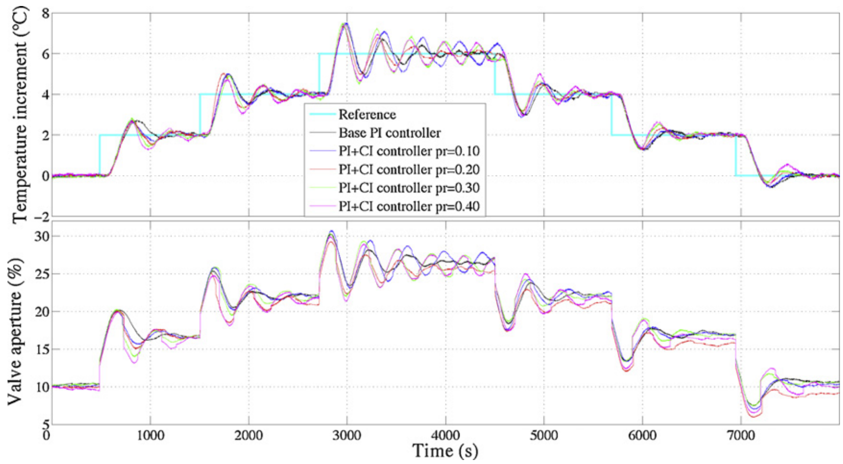


**Fig. 13.** Responses and control signals of base PI and PI+CI controllers.

**Table 3**
Performance indexes for the PI and PI+CI control systems.

| Controller | IAE (s) | ITAE ($s^2$) | Phase margin (°) |
|---|---|---|---|
| Base PI | $3.31 \times 10^3$ | $12.45 \times 10^6$ | 41 |
| PI+CI $p_{reset} = 0.1$ | $3.75 \times 10^3$ | $14.14 \times 10^6$ | 44 |
| PI+CI $p_{reset} = 0.2$ | $3.28 \times 10^3$ | $12.09 \times 10^6$ | 46 |
| PI+CI $p_{reset} = 0.3$ | $3.62 \times 10^3$ | $13.12 \times 10^6$ | 47 |
| PI+CI $p_{reset} = 0.4$ | $3.87 \times 10^3$ | $14.54 \times 10^6$ | 47 |

### *3.3. Reset compensation with reset band*

The reset action is a good choice to improve the transitory response of a closed loop system. But there are systems whose response improvement is not as good as it can be expected. This is due to the presence of a dominant time delay. The problem in these dominant time delay systems is that the reset action is done at reset times ($t_k$), when error is equal to zero, but the system suffers the reset action at another time, specifically at $t_k + h$, where $h$ is the time delay of the plant. This lack of coordination between the reset times and the times when the system undergoes the reset action can be overcome by modifying the reset condition.

The reset condition in the PI+CI controller has been usually given by the fact that the error signal had to be equal to zero. In this Section, the reset condition is modified with the goal of doing reset some time before the crossing between the error signal and zero. To specify when the reset action must exactly be done, two techniques are considered in this work: a fixed reset band and a variable reset band.

#### *3.3.1. Fixed reset band*

In this case, the new reset condition consists of doing reset when the error signal is approaching to zero and when the system output reaches some specified value. This value will be fixed by the parameter *r* eset band, $\delta$. With this new reset condition, the reset controller (4) is expressed in state space through the following expression [7]

$$C : \begin{cases} \dot{x}_r(t) = A_r x_r(t) + B_r e(t), & (e(t), \dot{e}(t)) \notin \mathcal{B}_\delta^f \\ x_r(t^+) = A_\rho x_r(t), & (e(t), \dot{e}(t)) \in \mathcal{B}_\delta^f \\ v(t) = C_r x_r(t) + D_r e(t) \end{cases} \tag{18}$$

where the fixed reset band surface $\mathcal{B}_\delta^f$ is defined as:

$$\mathcal{B}_\delta^f = \{(e(t), \dot{e}(t)) \in \mathbb{R}^2 | (e(t) = \delta \wedge \dot{e}(t) < 0) \vee (e(t) = -\delta \wedge \dot{e}(t) > 0)\} \tag{19}$$

This new condition establishes that the reset action takes place when the error signal reaches a fixed value, $\delta$, before crossing to zero. In this case, the reset surface is not the same hyperplane as in the original definition (6), but it consists of two reset lines $\mathcal{B}_\delta^{f+}$ and $\mathcal{B}_\delta^{f-}$, as it can be seen in Fig. 14.

When $\delta = 0$, the reset instant occurs at $e(t) = 0$ and then the reset controller is the original one (4). On the other hand, if $\delta$ is really large, the reset action will never take place, so that the reset controller is reduced to its lineal PI counterpart. Therefore, the choice of the reset band value is the key in the design of a PI+CI controller with fixed reset band.

In [7] the Clegg integrator describing function was computed with a fixed reset band

$$D_{CI}^\delta(E, \omega) = \frac{1}{j\omega}\left(1 + \frac{j4\sqrt{1-\left(\frac{\delta}{E}\right)^2}}{\pi} e^{j sin^{-1}\left(\frac{\delta}{E}\right)}\right) \tag{20}$$

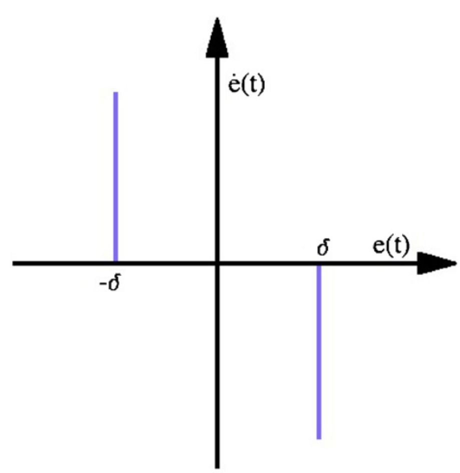


**Fig. 14.** Fixed reset band surface.

**Table 4**
Performance indexes for the PI and PI+CI control systems with fixed reset band.

| Controller | IAE (s) | ITAE ($s^2$) |
|---|---|---|
| PI-IMC | $2.59 \times 10^3$ | $9.56 \times 10^6$ |
| PI+CI $p_{reset} = 0.10$ and $\delta/E = 0.6$ | $2.16 \times 10^3$ | $8.17 \times 10^6$ |
| PI+CI $p_{reset} = 0.35$ and $\delta/E = 0.7$ | $2.82 \times 10^3$ | $10.86 \times 10^6$ |

where $E$ is the error amplitude. By replacing this equation into the PI+CI controller transfer function, the PI+CI describing function with fixed reset band is given

$$D^{\delta}_{PI+CI}(E,\omega) = k_p\left(1+\frac{1}{j\omega\tau_i}\left(1+\frac{j4p_{reset}\sqrt{1-\left(\frac{\delta}{E}\right)^2}}{\pi}e^{j\sin^{-1}\left(\frac{\delta}{E}\right)}\right)\right) \quad (21)$$

For comparison purposes, in Fig. 15 the Bode plot is shown for a PI controller ($k_p = \tau_i = 1$) and for a PI+CI one ($k_p = \tau_i = 1$ and $p_{reset} = 0.50$) with several fixed reset bands ($\delta/E = 0.25$, 0.50, 0.75 and 1.00).

It can be seen that the controller phase is increased with the fixed reset band for some values. Specifically, in this case, when $p_{reset} = 0.50$, the higher controller phase is obtained in a range $\delta/E \in [0.25, 0.50]$. This phase increment should make the delay effect less influential over the heat exchanger responses, by giving smaller overshoots and undershoots, and hence, smaller IAE and ITAE values.

The common experiment is carried out again, but now for two PI+CI controllers with fixed reset band. In this case, two different values of reset ratio are set and its corresponding fixed reset band are computed. In one controller, a low reset ratio is chosen and for this value, $p_{reset} = 0.1$, a fixed reset band has been computed with the goal of having the maximum phase margin in the control system. In this case, the maximum phase margin, 47°, has been obtained for a fixed reset band of $\delta/E = 0.6$. On the other hand, for a second PI+CI controller with fixed reset band, a higher reset ratio value is chosen, $p_{reset} = 0.35$. In this case, the control system reach the maximum phase margin, 60° when $\delta/E = 0.7$.

In Fig. 16, the heat exchanger responses and the control signals for these PI+CI controllers and for the PI-IMC controller are shown. In addition, its performance indexes are compared in Table 4.

From Fig. 16 and Table 4, it can be said that the PI+CI controller with $p_{reset} = 0.35$ and $\delta/E = 0.7$ in spite of having higher phase margin, its response it is not as good as the one given by the PI+CI controller with $p_{reset} = 0.1$ and $\delta/E = 0.6$. This last PI+CI controller not only has lower IAE and ITAE values than the other PI+CI controller, but it also has less overshoots and undershoots, in such a way that it gives the better response. In fact, this PI+CI controller response is also much better than the PI-IMC response, since it is faster and it has similar overshoots and undershoots with lower performance indexes.

However, as it can be seen from the control signals, the control system just undergoes the reset action once in each reference step with this new reset condition (19). Therefore, after the first and the only reset instant, the control system behaves as the lineal base PI controller and the goal of having a reset controller is not completely reached. So, in order to improve the system performance with reset action by doing more than one reset, a reset band which varies along the time will be considered in the next.

### 3.3.2. Variable reset band

Here, a variable reset band is considered to overcome the influence of the dominant time delay over the reset action. For that purpose, the same approach as in [17] is followed. In this case, the reset conditions are also given when the error signal is approaching to zero, but now, the value of the error when the reset action is done will change constantly from one reset instant to another one.

These constantly reset band changes will be predicted by using the error signal derivative. The derivative of a function at a chosen input value describes the best linear approximation of the function near that input value. In this way, the reset instants will be predicted by using the error signal derivative approximation. This approximation states that the error signal derivative at a point is equal to the slope of the tangent line to the graph of the error signal at that point. Therefore, the following expression is obtained

$$\tan\alpha = \frac{de(t)}{dt} = \frac{-e(t)}{h} \quad (22)$$

where $h$ is the time delay process. From this equation, the new variable reset condition is expressed as

$$h\frac{de(t)}{dt} + e(t) = 0 \quad (23)$$

As it can be seen, no parameter has to be fixed in this new condition, since the time delay $h$ is given by the process dynamics. With this new reset condition (23), the reset controller (4) is expressed now in the state-space as

$$C:\begin{cases}\dot{x}_r(t) = A_r x_r(t) + B_r e(t), & (e(t),\dot{e}(t)) \notin \mathcal{B}^{\nu}_h \\ x_r(t^+) = A_\rho x_r(t), & (e(t),\dot{e}(t)) \in \mathcal{B}^{\nu}_h \\ v(t) = C_r x_r(t) + D_r e(t) & \end{cases} \quad (24)$$

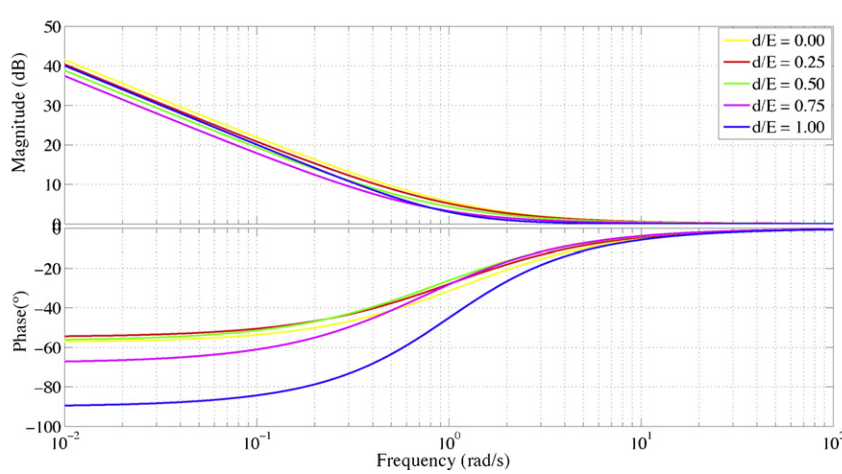


**Fig. 15.** Bode plots for PI+CI controller with several fixed reset bands.

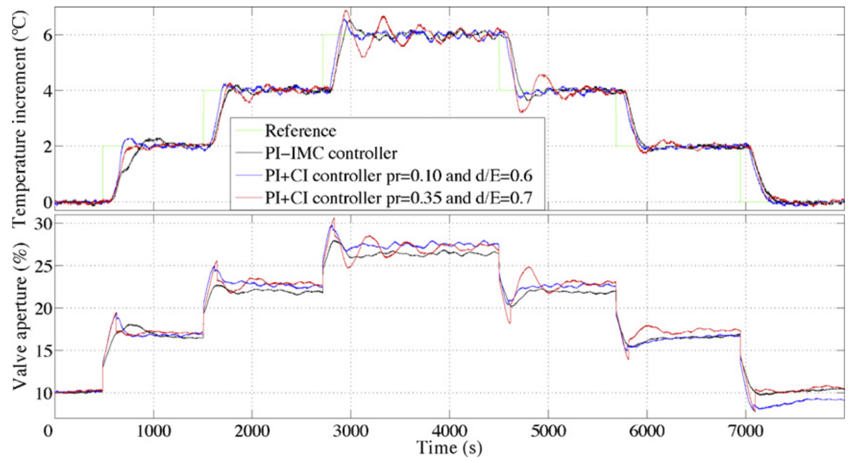


**Fig. 16.** Responses and control signals of PI-IMC and PI+CI controllers with fixed reset band.

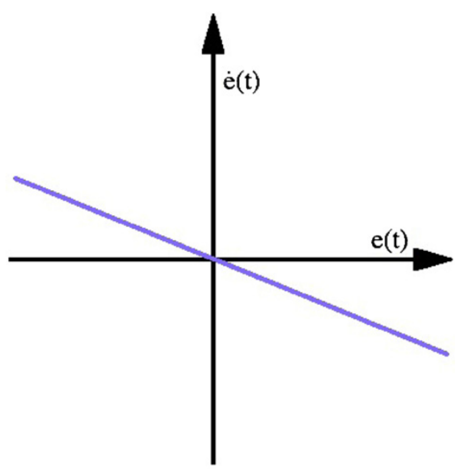


**Fig. 17.** Variable reset band surface.

where the variable reset band surface $\mathcal{B}_h^v$ is given by:

$$\mathcal{B}_h^v = \{(e(t), \dot{e}(t)) \in \mathbb{R}^2 | h\dot{e}(t) + e(t) = 0\} \quad (25)$$

In this case, the reset surface is a continuous function of the error signal, as it can be seen in Fig. 17. When there is no time delay, $h = 0$, the reset condition (25) is equal to the original one (6).

In the frequency domain, the Clegg integrator describing function describing function may be computed resulting in (details are omitted by brevity)

$$D_{\mathrm{CI}}^h(\omega) = \frac{1}{j\omega}\left(1 + \frac{j2}{\pi}(1 + e^{j2tan^{-1}(\omega h)})\right) \quad (26)$$

where $h$ is the time delay of the process. A similar result is given in [18]. By replacing this equation into the PI+CI controller transfer function, the PI+CI describing function with variable reset band is given

$$D_{\mathrm{PI+CI}}^h(\omega) = k_p\left(1 + \frac{1}{j\omega\tau_i}\left(1 + \frac{j2p_{\mathrm{reset}}}{\pi}(1 + e^{j2tan^{-1}(\omega h)})\right)\right) \quad (27)$$

This describing function can be used in this case as previously. That is, the phase margin system can be increased by setting the parameters $p_{\mathrm{reset}}$ and $h$ properly in the controller. This phase margin increment can make the heat exchanger performance improve, since the time delay is less influential over the heat exchanger responses when a variable reset band is present.

As it was said, just the nominal time delay has to be fixed in the variable reset band. For the industrial heat exchanger studied in this work, the time delay is uncertain and several values of time delay can be chosen. Theoretically, the reset instants are going to take place $h$ time units time before that the error signal crosses to zero. Therefore, in order not to degrade the response to any reference change, the nominal time delay is taken as the minimum one, that is, $h = 50$ s. In addition, due to the presence of sensor noise, the

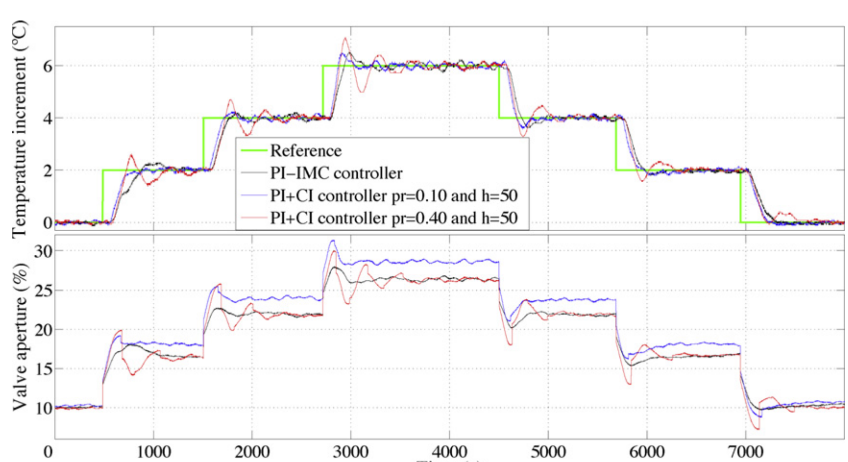


**Fig. 18.** Responses and control signals of PI-IMC and PI+CI controllers with variable reset band.

**Table 5**
Performance indexes for the PI and PI+CI control systems with variable reset band.

| Controller | IAE ($s$) | ITAE ($s^2$) |
|---|---|---|
| PI-IMC | $2.59 \times 10^3$ | $9.56 \times 10^6$ |
| PI+CI $p_{\text{reset}} = 0.1$ and $h = 50$ s | $2.13 \times 10^3$ | $8.09 \times 10^6$ |
| PI+CI $p_{\text{reset}} = 0.4$ and $h = 50$ s | $2.92 \times 10^3$ | $10.67 \times 10^6$ |

derivative part of this reset band will be filtered by a low pass filter with a constant time ten times smaller than the nominal time delay, that is, $\tau_f = 5$ s.

For comparison purposes, the same experiment explained previously is carried out at the same operation conditions. In this case, the PI-IMC controller response is compared to the PI+CI controller with variable reset band and two different reset ratios, $p_{\text{reset}} = 0.1$ and $p_{\text{reset}} = 0.4$. In Fig. 18, both the responses and the control signals are drawn for these three controllers. On the other hand, in Table 5, the IAE and ITAE values are computed.

In addition, phase margins are computed for the reset system with and without variable reset band by using (27). For the PI+CI controller without reset band, the phase margin is obtained as 61.5° and 67.1° for $p_{\text{reset}} = 0.1$ and $p_{\text{reset}} = 0.4$ respectively. When the variable reset band is considered, $h = 50$ s, these phase margins are increased up to 63° and 76.3° respectively, and hence a better performance can be expected.

From Fig. 18 and Table 5, it is deduced that the PI+CI controller with variable reset band and a reset ratio equals to $p_{\text{reset}} = 0.1$ is the best option to control the temperature increments in an industrial heat exchanger, since in comparison with the PI controller tuned with IMC, a faster response is obtained with more or less the same overshoot and undershoot. In this case, the PI+CI controller does several resets and not only just one, as with the fixed reset band. Therefore, it can be concluded that the variable reset band can be used to improve significantly the reset performance and the lineal IMC response when dominant time delays are present in the system dynamic.

## 4. Conclusions

Temperature control problem is studied here through the experimental control of an industrial heat exchanger. This work has investigated the potentials of a nonlinear/hybrid compensator (PI+CI) in the robust control of these types of processes. A two-step design technique has been carried out, based on the use of Quantitative Feedback Theory. It has been proved how two simple ideas, that is the partial reset of the integral term and the use of a reset band, can significantly improve closed loop performance, in spite of parametric uncertainty, in comparison with a PI controller tuned by using the Internal Model Control technique. All the results have been done by means of experimentation over an industrial heat exchanger commonly used in food industry. Note that although the work is tailored to a specific temperature control problem of an industrial heat exchanger, this method can be applied to any system in which a fast response with hardly overshoot is required.

Although this work is focused to first order plus time delay (FOPTD) systems, it can be applied to general systems with significant parametric uncertainty, since the QFT technique provides a general framework to approach robust control problems. The advantages of using reset compensation instead of LTI compensation are mainly due to the phase lead increment given by reset action with approximately the same magnitude. The improvement which can be obtained with reset compensation depends on every practical case, but in general some improvement can be always expected.

## Acknowledgements

This work was supported by the Spanish Department of Education and Science under project DPI2007-66455-C02-01.

## References

[1] R. Aguilar, S.A. Martínez, M.G. Rodríguez, G. Soto, Process analysis for treatment of industrial plating wastewater: simulation and control approach, Chemical Engineering Journal 105 (2005) 139–145.
[2] M. Alpbaz, S. Karacan, Y. Cabbar, H. Hapoğlu, Application of model predictive control and dynamic analysis to a pilot distillation column and experimental verification, Chemical Engineering Journal 88 (2002) 163–174.
[3] A. Altinten, F. Ketevanlioğlu, S. Erdoğan, H. Hapoğlu, M. Alpbaz, Self-tuning PID control of jacketed batch polystyrene reactor using genetic algorithm, Chemical Engineering Journal 138 (2008) 490–497.
[5] M.A. Arbaoui, L. Vernières-Hassimi, D. Seguin, M.A. Abdelghani-Idrissi, Counter-current tubular heat exchanger: Modeling and adaptive predictive functional control, Applied Thermal Engineering 27 (2007) 2332–2338.
[6] A. Baños, A. Barreiro, Delay-independent stability of reset control systems, IEEE Transactions on Automatic Control (2008).
[7] A. Baños, S. Dormido, A. Barreiro, Stability analysis of reset control systems with reset band, in: Proceedings of the 3rd IFAC Conference on Analysis and Design of Hybrid Systems 2009, Zaragoza, Spain, 16–18 September.
[8] A. Baños, P. Garcia, L. Checa, Robust control of thermal treatments in can industry, in: Proceedings of the 4th IFAC/CIGR Workshop - Control Appliations in Post - Harvest and Processing Technology (CAPPT 2006), Potsdam, Germany, 2006.
[9] A. Baños, A. Vidal, Design of PI+CI Reset Compensators for second order plants, pp. 118–123, in: Proceedings of the 2007 IEEE International Symposium on Industrial Electronics, Vigo, Spain, 4–7 June, 2007.
[10] A. Baños, A. Vidal, Definition and tuning of a PI+CI reset controller, pp. 4792–4798, in: Proceedings of the European Control Conference 2007, Kos, Greece, 2–5 July, 2007.
[11] A. Baños, O. Yaniv, F.J. Montoya, Nonlinear QFT synthesis by local linearization, International Journal of Control 76 (5) (2003) 429–436.
[12] O. Beker, Analysis of reset control systems, Ph.D. Thesis, University of Massachusetts Amherst, 2001.
[13] O. Beker, C.V. Hollot, Y. Chait, H. Han, Fundamental properties of reset control systems, Automatica 40 (2004) 905–915.
[14] G. Carrizales-Martínez, R. Fermat, V. González-Alvarez, Temperature control via robust compensation of heat generation: isoparaffin/olefin alkylation, Chemical Engineering Journal 125 (2006) 89–98.
[15] J. Cervera, Ajuste automático de controladores en QFT mediante estructuras fraccionales, Ph.D. Thesis, University of Murcia, Spain, 2006.
[16] J.C. Clegg, A nonlinear integrator for servomechnisms, Transactions A.I.E.E.m, Part II 77 (1958) 41–42.
[17] A. Fernández, A. Barreiro, A. Baños, J. Carrasco, Reset control for passive teleoperation, pp. 2935–2940, in: Proceedings of the 34th Annual Conference of the IEEE Industrial Electronics Society, Orlando, USA, 10–13 November, 2008.
[18] A. Fernández, A. Barreiro, A. Baños, J. Carrasco, Reset control for passive bilateral teleoperation, Post-IECON of the IEEE Transactions on Industrial Electronics, submitted for publication.
[19] M. Fischer, O. Nelles, R. Isermann, Adaptive predictive control of a heat exchanger based on a fuzzy model, Control Engineering Practice 6 (1998) 259–269.
[20] Y. Guo, Y. Wang, L. Xie, J. Zheng, Stability analysis and design of reset systems: theory and an application, Automatica 45 (2009) 492–497.
[21] I.M. Horowitz, Quantitative Feedback Theory, QFT Press, 1992.
[22] I.M. Horowitz, Rosenbaum, Nonlinear design for cost of feedback reduction in systems with large parameter uncertainty, International Journal of Control 24 (6) (1975) 977–1001.
[23] K.R. Krishman, I.M. Horowitz, Synthesis of a nonlinear feedback system with significant plant-ignorance for prescribed system tolerances, International Journal of Control 19 (4) (1974) 689–706.
[24] S. Karacan, H. Hapoğlu, M. Alpbaz, Application of optimal adaptive generalized predictive control to a packed distillation column, Chemical Engineering Journal 84 (2001) 389–396.
[25] I.D. Landau, System Identification and Control Design, Prentice Hall, 1990.
[26] Y. Lee, S. Park, M. Lee, C. Brosilow, PID controller tuning for desired closed-loop responses for SI/SO systems, American Institute of Chemical Engineers Journal 44 (1) (1998) 106–115.
[27] Z. Loulch, M. Cabassud, M.V. Le Lann, A new strategy for temperature control of batch reactors: experimental application, Chemical Engineering Journal 75 (1999) 11–20.
[28] A. Maidi, M. Diaf, J.P. Corriou, Optimal linear PI fuzzy controller design of a heat exchanger, Chemical Engineering and Processing 47 (2008) 938–945.
[29] D.E. Rivera, M. Morari, S. Skogestad, Internal model control. 4. PID controller design, Industrial and Engineering Chemistry Process Design and Development 25 (1) (1986) 252–265.
[30] S. Skogestad, Simple analytic rules for model reduction and PID controller tuning, Journal of Process Control 13 (4) (2003) 291–309.

[31] C.L. Smith, A.B. Corripio, J. Martin, Controller tuning from simple process models, Instrumentation Technology 22 (12) (1975) 39–44.
[32] A. Vidal, A. Ba-os, Stability of reset control systems with variable reset: application to PI+CI compensation, pp. 4913–4918, in: Proceedings of the European Control Conference 2009, Budapest, Hungary, 23–26 August, 2009.
[33] L. Zaccarian, D. Nešić, A.R. Teel, First order reset elements and the Clegg integrator revisited, pp. 563–568, in: American Control Conference, Portland (OR), USA, 2005.
[34] J. Zheng, Y. Guo, M. Fu, Y. Wang, L. Xie, Development of an extended reset controller and its experimental demonstration, IET Control Theory and Applications 2 (2008) 866–874.